

Submission to International Journal of Cosmetic Science

17/12/2014

1 **The Occlusion Effects in Capacitive Contact Imaging for *In-vivo* Skin Damage**
2 **Assessments**

3

4 Wei Pan¹, Xu Zhang¹, Majella Lane² and Perry Xiao^{1*}

5

6 ¹School of Engineering, London South Bank University, 103 Borough Road, London

7 SE1 0AA, United Kingdom

8 ²UCL School of Pharmacy, 29-39 Brunswick Square, London WC1N 1AX, United

9 Kingdom

10

11 * Corresponding Author, Tel: 00 44 20 7815 7569 Fax: 00 44 20 7815 7561

12 email: xiaop@lsbu.ac.uk

13

14 **Abstract**

15 **OBJECTIVE:** The aim of this study is to investigate the occlusion effects in

16 capacitive contact imaging, in order to develop a new quantitative methodology for

17 *in-vivo* skin assessments by using capacitive contact imaging and

18 condenser-TEWL(trans-epidermal water loss) method.

19

20 **METHODS:** Two measurement technologies are used in this study, i.e. capacitive
21 contact imaging and condenser-TEWL method. Three types of skin damages are
22 studies, intensive washes and tape stripping, and sodium lauryl sulfate (SLS)
23 irritation. The test skin sites were choose on the volar forearms of healthy
24 volunteers (aged 25 - 45), the measurements were performed both before and
25 periodically after the damages.

26

27 **RESULTS:** The results show that the time-dependent occlusion curves of
28 capacitive contact imaging can reflect the types of damages, and by analysing the
29 shapes of the curves we can get information about the skin surface water content
30 level and stratum corneum thickness. The results also show that the combination of
31 capacitive contact imaging and condenser-TEWL method gives extra information
32 about the skin damages.

33

34 **CONCLUSION:** We have developed a potential new quantitative methodology for
35 skin damage assessments by using capacitive contact imaging and
36 condenser-TEWL method. The combination of the two technologies can provide
37 useful information for skin damage assessments. We have also developed a
38 mathematical model for analysing the occlusion curves.

39

40 **Keywords**

41 Skin occlusion, capacitive contact imaging, skin damage assessments, skin
42 hydration, TEWL.

43

44 **1. Introduction**

45 Skin damage is a very important issue for occupational health as well as
46 environmental threat [1,2]. However, to assess the skin damage is not easy,
47 especially quantitatively. To date, skin damage assessments are largely done
48 through visual assessments, which can be subjective and difficult to quantify. There
49 is a need to develop a new, quantitative, and simple methodology that can quantify
50 the skin damage assessments. We know that water in stratum corneum (SC) plays
51 an important role in skin's cosmetic properties as well as its barrier functions, and
52 SC water concentration and trans-epidermal water loss (TEWL) are two key
53 indexes for skin characterizations [3,4]. In this paper, we present our latest study on
54 the occlusion effects in capacitive contact imaging for *in-vivo* skin damage
55 assessments. Capacitive contact imaging based fingerprint sensors, originally
56 designed for biometric applications, has shown potential for skin hydration imaging,
57 surface analysis, 3D surface profile, skin micro-relief as well as solvent penetration

58 measurements [5-11]. With the capacitive contact imaging, we can measure the
59 skin surface water concentration distribution map. By occluding the skin with
60 capacitive imaging sensor over a period of time, as water dynamically builds up
61 underneath the sensor surface due to the blockage of trans-epidermal water loss,
62 we can also generate time-dependent skin occlusive hydration curves. It is this
63 time-dependent occlusive hydration curves that we are mainly interested in this
64 study. Our previous studies have also shown that skin occlusion measurements can
65 give further information about skin properties [12]. The purpose of this study is to
66 develop a new methodology for skin damage assessments by using skin capacitive
67 contact imaging occlusion measurements, as well as the trans-epidermal water loss
68 (TEWL) measurements.

69

70 **2. Materials and Methods**

71 2.1 Instruments

72 The capacitive contact imaging technology developed by the research group [8-11]
73 is based on Fujitsu fingerprint sensor (Fujitsu Ltd, Japan), which has a matrix of 256
74 × 300 pixels, with 50 μm spatial resolution per pixel. The fingerprint sensor basically
75 generates capacitance images of the skin surface. In each image, each pixel is
76 represented by an 8 bit grayscale value, 0~255, higher grayscale values mean

77 higher water concentration, and lower grayscale values mean lower water
78 concentration.

79

80 The TEWL measurements were performed by using the condenser-TEWL method
81 (AquaFlux, Biox Systems Ltd, UK), which is a condenser based closed-chamber
82 measurement technology [13,14]. Its cylindrical measurement chamber is open at
83 the end placed onto the skin surface, and closed by means of a condenser cooled
84 below the freezing temperature of water at the other end. This design provides a
85 controlled measurement environment, which enhances the repeatability and
86 accuracy of the measurements.

87

88 2.2 Mathematical Modeling of Skin Occlusion

89 According to diffusion theory, the skin occlusion can be described by following one
90 dimensional diffusion equation with following initial condition and boundary
91 condition.

92

$$93 \quad \begin{cases} D(H) \frac{\partial^2 H}{\partial z^2} = \frac{\partial H}{\partial t}, & 0 \leq z \leq L \\ H(z, 0) = f(z) \\ H(L, t) = H_1 \\ -D \frac{\partial H}{\partial z} \Big|_{z=0} = 0 \end{cases} \quad (1)$$

94

95 where $H(z,t)$ is the skin water content at depth z and time t , L is SC thickness, $D(H)$
 96 is the SC water diffusion coefficient, which is a function of water content $H(z,t)$, $f(z)$
 97 is the initial skin water distribution within SC. In this case, we can assume it is a
 98 linear distribution, defined by

$$99 \quad f(z) = H_0 + \frac{H_1 - H_0}{L} \times z. \quad (2)$$

100 where H_0 is the SC surface water concentration, and H_1 is the SC bottom water
 101 concentration. In Eq.(1), at the skin surface ($z=0$), there is zero flux due to occlusion,
 102 and at the SC bottom ($z=L$), we assume there is a constant water concentration H_1 .

103 We can solve the Eq.(1) by substituting Eq.(2) into Eq.(1), and the solution can be
 104 expressed as,

105

$$106 \quad H(z, t) = H_1 + \frac{2}{L} \sum_{n=0}^{\infty} \left(e^{-\frac{D(2n+1)^2 \pi^2 t}{4L^2}} \times \cos \frac{(2n+1)\pi z}{2L} \times \left(\frac{2L(-1)^{n+1} H_1}{(2n+1)\pi} + \right. \right.$$

$$107 \quad \left. \left. \frac{2L(H_1(2n+1)\pi \cos(n\pi) + 2(H_1 - H_0)(1 + \sin(n\pi)))}{(2n+1)^2 \pi^2} \right) \right)$$

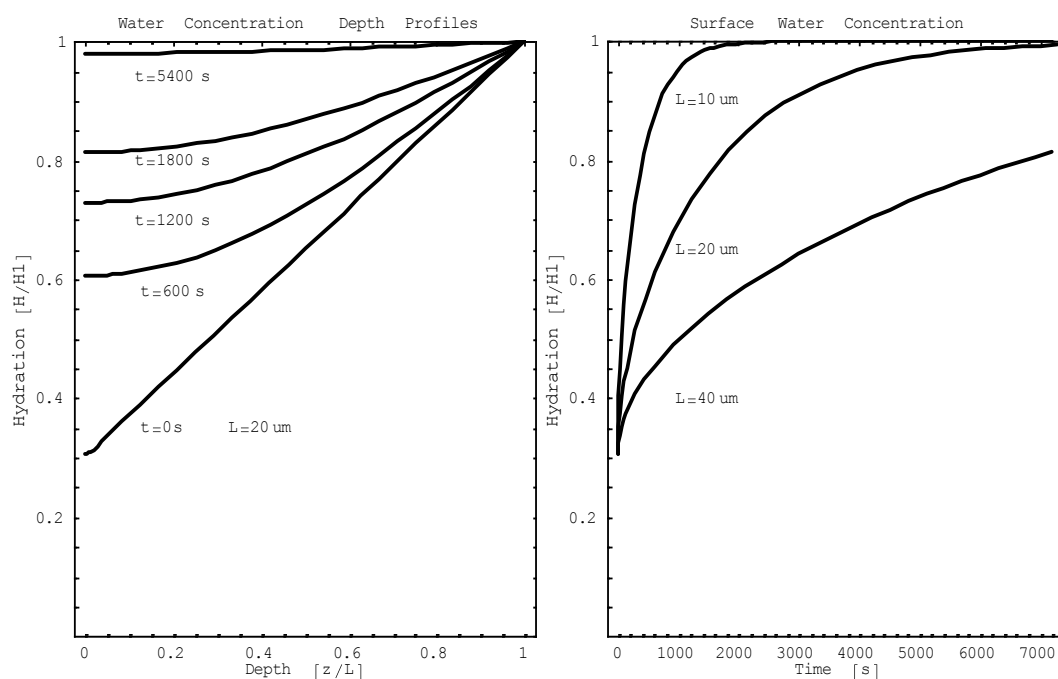
108 (3)

109

110 Figure 1 shows results of above solution, the left plot shows the SC water
 111 concentration depth profiles at different time during the occlusion, using normalized
 112 the depth (z/L , $L=20\mu\text{m}$) and normalized water concentration (H/H_1 , $H_1=80\%$
 113 $H_0=24\%$), and right plot shows the time dependent normalized surface water

114 concentration (H/H_1 , $H_1=80\%$ $H_0=24\%$) levels of three different SC thickness
 115 ($L=10\mu\text{m}$, $20\mu\text{m}$, $40\mu\text{m}$).

116



117

118 Figure 1 The SC normalized water concentration depth profiles at different time
 119 during the occlusion with $L=20\mu\text{m}$ (left), and the time dependent normalized surface
 120 water concentration levels of three different SC thickness (right).

121

122 The results show that different SC thicknesses have different times to reach steady
 123 state, for a SC with $20\mu\text{m}$ thickness, which is typical SC thickness in volar forearm,
 124 it is about 30 minutes to reach 80% of H_1 and about 2 hours to reach the steady
 125 state, i.e. 100% of H_1 .

126

127 2.3 Experimental Procedures

128 In this paper, skin sites on volar forearms of healthy volunteers, aged 25 - 45, were
129 chosen for the measurements. The skin test sites were deliberately damaged by
130 intensive washes, tape stripping and sodium lauryl sulfate (SLS) irritation. Intensive
131 washing used room temperature running water and washing-up liquid, rubbing the
132 site gently for 3 minutes with a finger. Tape stripping was performed 20 times per
133 site by the use of standard stripping tape. SLS irritation was achieved by applying
134 2% SLS solution (w/w) on skin. Capacitive contact imaging measurements and
135 TEWL measurements were performed both before and after the skin was damaged.
136 The skin occlusion measurements using capacitive contact imaging to occlude the
137 skin test sites for a period of one minute, during which skin capacitance images
138 were recorded continuously. The average grayscale values of the images were then
139 calculated at different times during occlusion. Since grayscale values are
140 proportional to SC hydration [8,11], the plots of grayscale value against time, can be
141 interpreted as SC hydration against time.

142

143 All the measurements were performed under normal ambient laboratory conditions,
144 of 20-21°C, and 40-50% RH. The volar forearm skin sites used were initially wiped

145 clean with ETOH/H₂O (95/5) solution. The volunteers were then acclimatized in the
146 laboratory for 20 minutes prior to the experiments.

147

148 **3 Results and Discussions**

149 3.1 The Occlusion Curves

150 Figure 2 shows capacitive contact imaging occlusion curves and corresponding
151 TEWL results of intensive wash, tape stripping and SLS irritation measurements.

152 The intensive washes produced small changes in the shapes of the contact imaging

153 occlusion curves. The general higher grayscale values of the occlusion curve

154 immediately after the washes indicate general higher SC hydration levels, which

155 may be caused by two factors, namely (i) superficial absorption of the water used in

156 the washes, and (ii) the removal of superficial SC cells during washing. After 25

157 minutes recovery time, the average grayscale values were found to have returned

158 to near-normal level. However, there is an undershoot, which suggests a

159 dehydration after the intensive washes, possibly due to the removal of some

160 superficial SC cells and the resultant loss of some SC barrier function. The TEWL

161 results follow a similar trend, and also confirmed the undershoot.

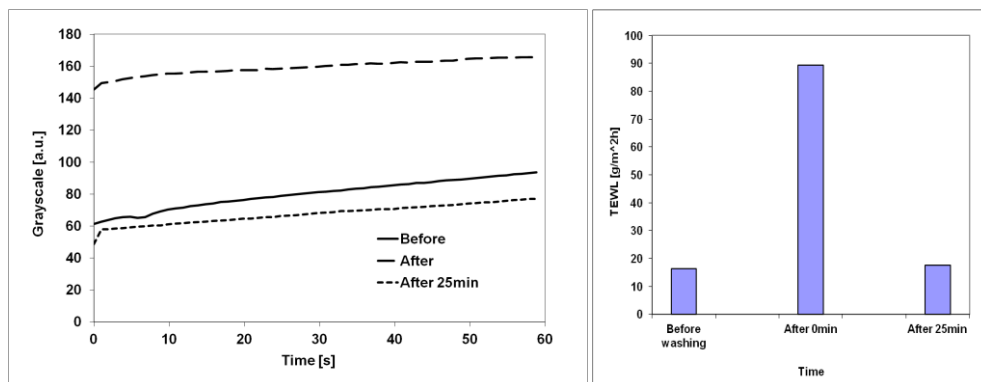
162

163 In tape stripping, the time dependent contact imaging occlusion curves show a
164 significant difference in shape (i.e. more curvature) between normal skin and
165 damaged skin. This curvature change reflects the SC structure change due to tape
166 stripping. Even after 60 minutes, the contact imaging occlusion curves were found
167 to be still significantly different from those of normal skin, indicating that SC was still
168 damaged. The TEWL values, however, has started returning to its normal value
169 after 60 minutes, indicating that although SC is still damaged, it starts to recover.

170

171 In SLS irritation, both the contact imaging occlusion curve and TEWL value
172 changed after irritation, but largely recovered after 40 minutes. It is interesting to
173 point out that the three types of skin damages produce three distinctive occlusion
174 curves, which indicates that, according to our theoretical modeling, the SC surface
175 hydration and SC structure are quite different under the different types of skin
176 damages. This suggests that the shapes of capacitive contact imaging occlusion
177 curves can provide extra information about skin damages. The results also show
178 that TEWL results can reflect the skin damages, but can not differentiate the
179 damages. Therefore, the combination of capacitive contact imaging occlusion
180 measurements and TEWL measurements can provide more detailed,
181 comprehension information about skin damages.

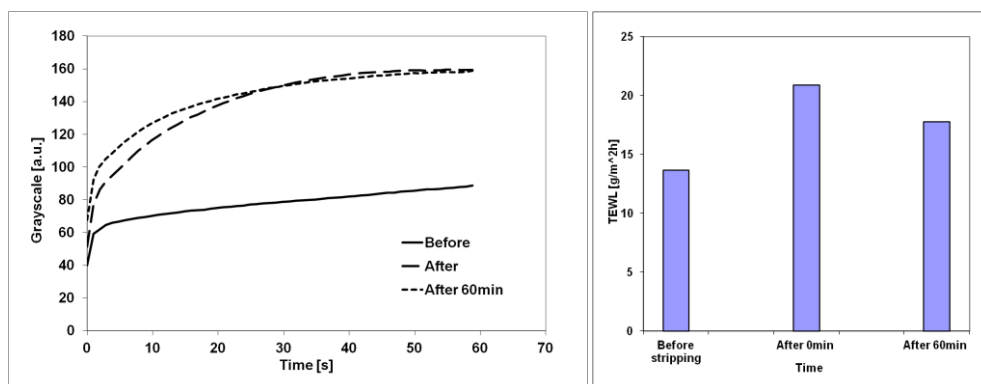
182



183

184

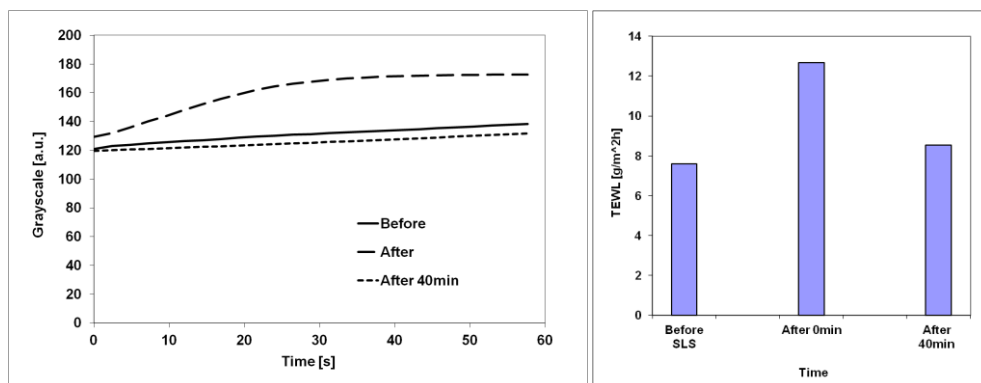
(a)



185

186

(b)



187

188

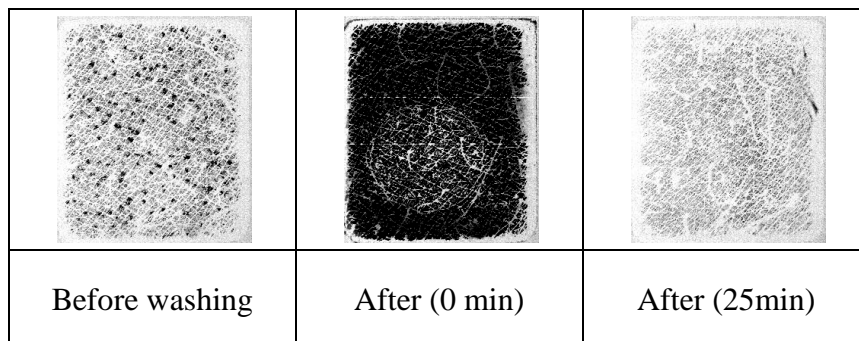
(c)

189 Figure 2. Skin capacitive contact imaging occlusion curves and corresponding

190 TEWL results of intensive washing (a); tape stripping (b); and SLS irritation (c).

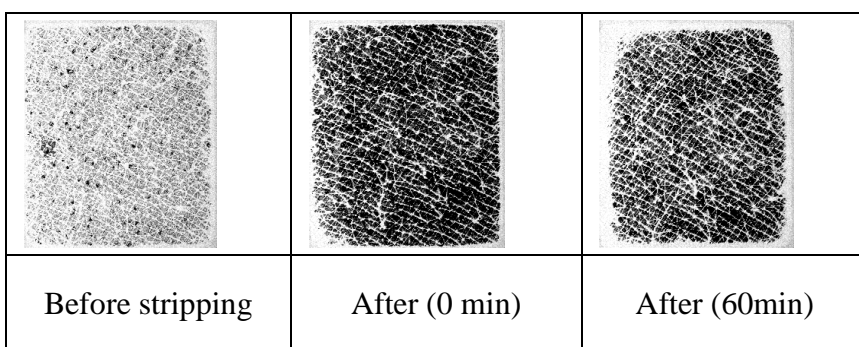
191

192



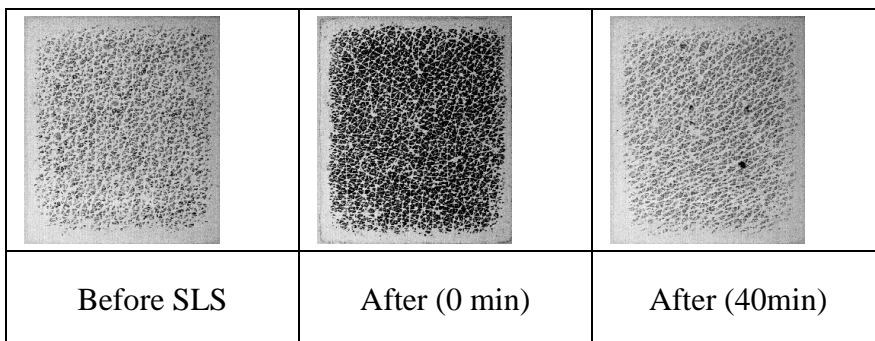
193

(a)



194

(b)



195

(c)

196 Figure 3 Skin capacitive contact images of intensive washes (a); tape stripping (b);

197 and SLS irritation (c).

198

199 Figure 3 shows corresponding capacitive contact images of intensive wash, tape

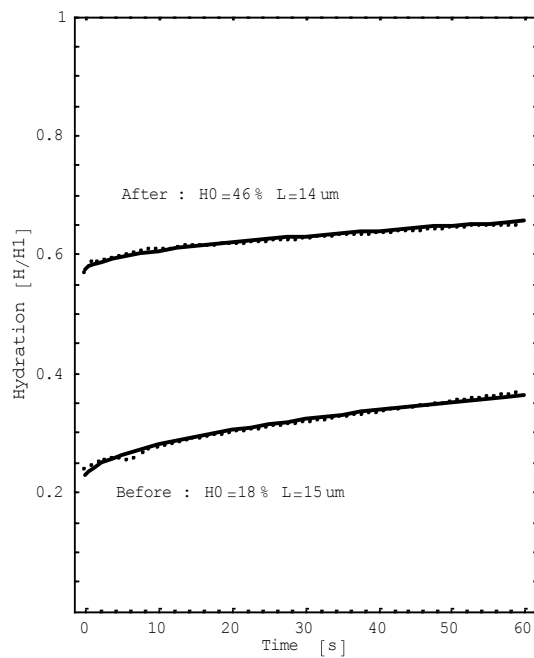
200 stripping and SLS irritation measurements. The skin images are generally getting

201 darker after damage, which indicates higher water content in SC. In both intensive
202 washes and SLS irritation, the lighter recovery skin images indicate there is a drying
203 effect after the damage. The lighter areas in the images immediately after the
204 intensive washing are imprints from the TEWL measurement head.

205

206 3.2 Comparison of Theoretical and Experimental Results

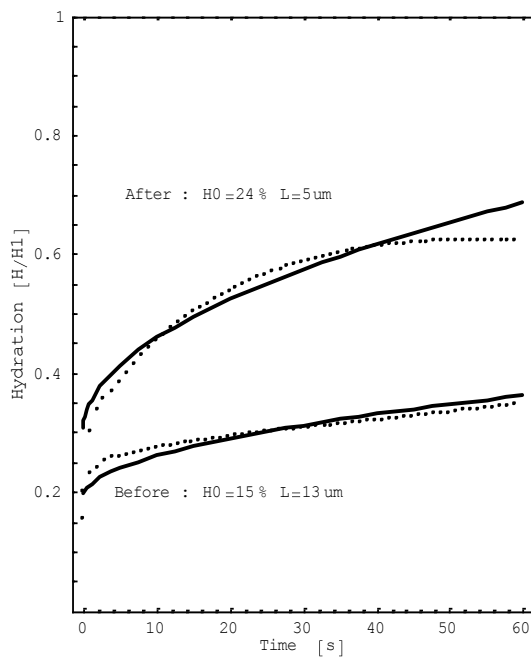
207 If we assume the maximum grayscale representing 100% water content, and zero
208 grayscale represent 0% water content, then we can compare the theoretical results
209 using Eq.(3) with above experimental results, see Figure 4. The comparison results
210 show that the intensive washing has significantly increased the SC surface water
211 content, but only slightly reduced the SC thickness, whilst the 20 tape stripping only
212 slightly increase the SC surface water content, but significantly reduced the SC
213 thickness. It is worth mentioning that the reduced SC thickness in theoretical
214 modeling data after SLS irritation is more likely to reflect the changes of water
215 distribution in SC, rather than the changes of SC structure. Overall, the theoretical
216 data matches better with normal skin data, the significant mismatch of theoretical
217 data and the data after 20 tape stripping, indicate that tape stripping has
218 significantly changed the structure of the SC.



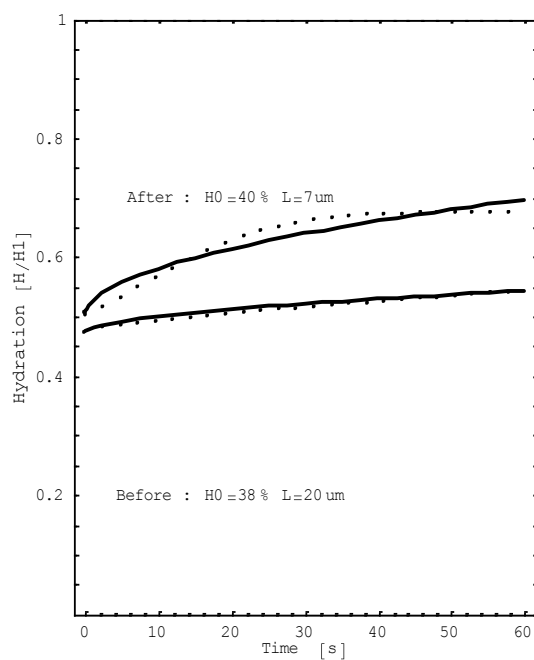
219

220

(a)



(b)



221

222

(c)

223 Figure 4 The comparison of theoretical results and experimental results, the

224 intensive washing (a), the tape stripping (b), and SLS irritation (c).

225

226 Clearly, whence the capacitive contact imaging is calibrated, we will be able to get
227 the SC surface content and SC thickness values by analysing the experimental
228 results using mathematical model described in Eq.(3).

229

230 **4 Conclusions and Future Works**

231 We have studied the occlusion effect in capacitive contact imaging for skin damage
232 assessments. The results show that the shapes of the capacitive contacting
233 imaging occlusion curves can be related to skin conditions, and different types of
234 skin damages have different shapes of occlusion curves. The TEWL measurements
235 can reflect the skin damages but can not differentiate different types of damages.
236 Therefore, the combination of skin occlusions using capacitive contact imaging and
237 TEWL measurements can provide useful, complementary information about skin
238 damage, and have potential as a new methodology for *in-vivo* skin damage
239 assessments. We have also developed a mathematical model for the skin occlusion,
240 the comparison of theoretical data and experimental data shows that the intensive
241 washes changes more of the SC surface water content, and the tape stripping
242 changes more of the SC thickness. The future work will be comparing the capacitive
243 contact imaging and TEWL measurements with other skin assessment

244 technologies, and to calibrate the capacitive contact imaging results, in order to

245 quantify the skin damage.

246

247 **Acknowledgement**

248 We thank London South Bank University for the financial support.

249

250 **References**

251 1. Dunitz M., The Environmental Threat to the Skin, Mark R and Plewig G (Ed.), The
252 University Press, Cambridge, ISBN 1-85317-057-7, 1992.

253 2. Grandjean P., Skin Penetration – Hazardous Chemicals at Work, Taylor &
254 Francis, London, ISBN 0-85066-834-4, 1990.

255 3. Fluhr J., Elsner P., Berardesca E., Maibach H.I. (Ed), Bioengineering of the Skin,
256 CRC Press, ISBN 0-8493-8374-9, 1995.

257 4. Fluhr J., Elsner P., Berardesca E., Maibach H.I. (Ed), Bioengineering of the Skin,
258 2nd Ed, CRC Press, ISBN 0-8493-1443-7, 2004.

259 5. Leveque, J.L. and Querleux, B. SkinChip, a new tool for investigating the skin
260 surface in vivo. Skin Research and Technology 9, 343-347, (2003).

261 6. Batische, D., Giron F. and Leveque J.L. Capacitance imaging of the skin surface.
262 Skin Research and Technology 12, pp99-104, (2006).

263 7. Bevilacqua, A., Gherardi, A., Guerrieri, R., "In Vivo Quantitative Evaluation of
264 Skin Ageing by Capacitance Image Analysis", IEEE Workshop on Applications of

- 265 Computer Vision and the IEEE Workshop on Motion and Video Computing
266 (WACV-MOTION), 2005, pp. 342-347, doi:10.1109/ACVMOT.2005.61
- 267 8. Xiao P, Singh H, Zheng X, Berg EP, Imhof RE, In-vivo Skin Imaging For
268 Hydration and Micro Relief Measurements. SCV Conference, Cardiff, UK, July
269 11-13, 2007.
- 270 9. Singh H, Xiao P, Berg P and Imhof RE, Skin Capacitance Imaging for Surface
271 Profiles and Dynamic Water Concentration Measurements, ISBS Conference,
272 Seoul, Korea, May 7-10, 2008.
- 273 10. Ou X, Pan W, Xiao P, In vivo skin capacitive imaging analysis by using grey
274 level co-occurrence matrix (GLCM), International Journal of Pharmaceutics,
275 November 2013, ISSN 0378-5173,
276 <http://dx.doi.org/10.1016/j.ijpharm.2013.10.024>.
- 277 11. Xiao, P., Ou, P., Ciortea, L.I., Berg E.P., and Imhof, R.E., "In-vivo Skin Solvent
278 Penetration Measurements Using Opto-thermal Radiometry and Fingerprint
279 Sensor", International Journal of Thermophysics, 33:1787–1794, DOI
280 10.1007/s10765-012-1318-6, 2012.
- 281 12. Taylor, H., New Techniques for Occupational Skin Health Surveillance, PhD
282 Thesis, London South Bank University, 2008.

- 283 13. Berg, E.P., Pascut, F.C., Ciortea, L.I., O'Driscoll, D., Xiao, P. and Imhof, R.R.
284 AquaFlux - A New Instrument for Water Vapour Flux Density Measurement,
285 Proceedings of the 4th International Symposium on Humidity and Moisture,
286 Center for Measurement Standards, ITRI, RoC, ISBN 957-774-423-0, 288-295,
287 (2002).
- 288 14. Imhof RE, De Jesus MEP, Xiao P, Ciortea LI and Berg EP, "Closed-chamber
289 transepidermal water loss measurement: microclimate, calibration and
290 performance", International Journal of Cosmetic Science, 31, 97–118, 2009.